European Radiology (2019) 29:5655–5663
https://doi.org/10.1007/s00330-019-06040-y

VASCULAR-INTERVENTIONAL

Early detection with MRI of incomplete treatment of spine metastases after percutaneous cryoablation

Guillaume Gravel[1] · Lambros Tselikas[1] · Benjamin Moulin[1] · Steven Yevich[1] · Eric Baudin[2] · Antoine Hakime[1] · Salma Moalla[1,3] · Fadila Mihoubi[3] · Corinne Balleyguier[3] · Thierry de Baere[1] · Frederic Deschamps[1]

Received: 9 October 2018 / Revised: 27 December 2018 / Accepted: 24 January 2019 / Published online: 15 March 2019

Abstract

Objectives To evaluate post-ablation MRI for the detection of incompletely treated spinal osseous metastases (SOM) after cryoablation and to propose a post-ablation imaging classification.

Methods After IRB consent, all patients treated with cryoablation of SOM between 2011 and 2017 having at least 1-year minimum follow-up and a spine MRI within 4 months after cryoablation were retrospectively included. A classification of MRI images into four types was set up. The primary endpoint of our study was to assess the diagnostic performance of the post-ablation MRI. The secondary endpoints were the 1-year complete treatment rate (CTR) and complications.

Results Fifty-four SOMs in 39 patients were evaluated. Post-ablation MRI was performed with a median delay of 25 days after cryoablation. Images were evaluated by two independent readers according to the pre-established image classification. Sensitivity and specificity for the detection of residual tumor were 77.3% (95%CI = 62.2–88.5) and 85.9% (95%CI = 75.0–93.4), respectively. Types I, II, III, and IV of the classification were associated with a 1-year complete treatment in 100%, 83.3%, 35.7%, and 10% of cases, respectively. The 1-year CTR was 59.3% for all 54 metastases, and 95.8% for metastases measuring less than 25 mm and at least 2 mm or more away from the spinal canal. Two grade 3 and two grade 2 adverse events according to the CTCAE were reported.

Conclusions MRI after cryoablation is useful for the evaluation of the ablation efficacy. The classification of post-cryoablation MRI provides reliable clues for the prediction of complete treatment at 1 year.

Key Points

- *MRI performed 25 days after cryoablation is useful to evaluate the efficacy.*
- *The proposed classification provides a reliable clue for complete cryoablation.*
- *Percutaneous cryoablation of spinal metastases is highly effective for lesions less than 25 mm in diameter and of at least 2 mm away from the spinal canal.*

Keywords Cryotherapy · Neoplasm metastasis · Spine · Magnetic resonance imaging

Abbreviations

CTR	Complete treatment rate
PMMA	Polymethylmethacrylate
SOM	Spinal osseous metastases
SBRT	Stereotactic body radiotherapy

✉ Guillaume Gravel
guillaume.gravel@gustaveroussy.fr

[1] Department of Interventional Radiology, Gustave Roussy Cancer Center, 114 rue Edouard Vaillant, 94805 Villejuif, France

[2] Department of Nuclear Medicine and Endocrine Oncology, Gustave Roussy Cancer Center, 114 rue Edouard Vaillant, 94805 Villejuif, France

[3] Department of Diagnostic Radiology, Gustave Roussy Cancer Center, 114 rue Edouard Vaillant, 94805 Villejuif, France

Introduction

Metastases to the axial skeleton are common in cancer patients [1, 2] and can induce devastating clinical consequences, including pain and immobility. They are related to the destruction of load-bearing vertebral components or extrinsic compression upon the spinal cord or neuroforaminal nerves [1] and are referred to as vertebral related events. Treatment for spinal metastatic disease requires a multidisciplinary approach.

Percutaneous cryoablation with cross-sectional imaging guidance is an appealing option as it provides reliable ablation zone, has the potential to monitor ablation margins during the procedure, and is minimally invasive, with generally well-tolerated pain. Instillation of compressed argon gas through the probes creates an extreme cold along the tip to temperatures less than minus 130 °C that results in local tissue necrosis [3, 4]. Cryoablation is a valid local treatment of bone metastases for local control, pain palliation, and prevention of skeletal-related events [3, 5, 6].

Ablation may also induce collateral damage to adjacent trabeculated bone, exposing to compression fracture and associated back pain. To prevent this sequela, cement vertebroplasty may be considered [4, 5]. It is usually performed as a subsequent procedure, and not immediately after the cryoablation, as the recently cryoablated bone retains hypothermic temperature and the distribution of injected polymethylmethacrylate (PMMA) could be non-uniform.

When local curative treatment is warranted, early detection of residual malignancy is useful as it might be re-treated, based on the probability that the residual is small and hopefully accessible to local treatment. Also, vertebroplasty before confirmation of completely local control may be problematic as it could preclude future access for a subsequent ablation and hamper early detection of such residual tumor. Therefore, a timely confirmation of tumor control is valuable for clinical management.

The sensitivity of MRI for the detection of bone metastases is high [7–9]. However, reports on early detection of incomplete treatment after spine cryoablation with imaging are scarce.

The aim of our study was to assess the performances of MRI after cryoablation of spine metastases for early detection of incomplete treatment.

Materials and methods

Data collection

We retrospectively retrieved all patients treated by percutaneous cryoablation for spine metastases to the vertebral body in our single institution cancer center from April 2011 to May 2017. Patient records were reviewed for patient demographics, primary tumor site, treatment course, number and size of metastases ablated, cryoablation modalities, proximity to the spinal canal, cortical bone erosion, soft tissue involvement, and procedural complications. Informed consent of patients for this study was waived by our local IRB. All patients had given the informed consent before the cryoablation was performed. Our institutional rules also stipulate that patients sign an agreement for future and retrospective analysis of anonymized data from their records.

Selection criteria

Inclusion criteria were (1) histologically confirmed diagnosis of metastatic cancer, (2) treatment by percutaneous cryoablation for local curative purpose of a spine metastasis, (3) minimum follow-up of 1 year, and (4) availability of spine MRI within 4 months after cryoablation.

Exclusion criteria were (1) cement injection in the treated vertebra prior to the post-ablation MRI and (2) absence of gadolinium chelates-enhanced T1-weighted sequence with fat saturation in the post-ablation MRI protocol.

Procedures

All procedures were performed with image guidance using CT or fluoroscopy with Cone Beam CT by a senior interventional radiologist. Procedures were performed either under general anesthesia or conscious sedation with lower extremity neurological monitoring. Epidural injection of carbon dioxide to displace the spinal cord or foraminal nerve root was performed on a case-by-case basis depending on proximity to the anticipated ablation zone. Pre-procedural medullar arteriography was performed on a case-by-case basis to localize the arteria radicularis magna depending on the vertebra treated and if the metastasis was in a position where the ablation zone might potentially overlap this vital structure. All cryoablation procedures were performed using the same system (Visual-ICE™ Cryoablation System, Galil Medical). The cryoablation probe number and size (IceSeed®, IceSphere®, and IceRod®) and probe positioning were selected on the basis of tumor size, location in the vertebral body, and proximity to the spinal canal or foramen. The treatment protocol used in our center for bone cryoablation is the following: two 10-min freeze cycles separated by a 9-min passive thaw and a 1-min active thaw.

Assessment

All post-ablation imaging examinations at 1 year were reviewed to establish the complete or incomplete ablation status. Local control failure was defined as a radiographic increase of the treated lesion on CT and/or MRI, and/or abnormal ^{18}F-FDG PET/CT uptake. If one of those three examinations was positive, the ablation was considered incomplete.

Post-ablation MRI was first analyzed by a senior radiologist with knowledge of the 1-year complete history. The goal of this first evaluation was to define the different post-ablation MRI patterns and to formulate a comprehensive new classification.

Based on the post-ablation MRI patterns, four MRI appearance types were established as follows (Fig. 1):

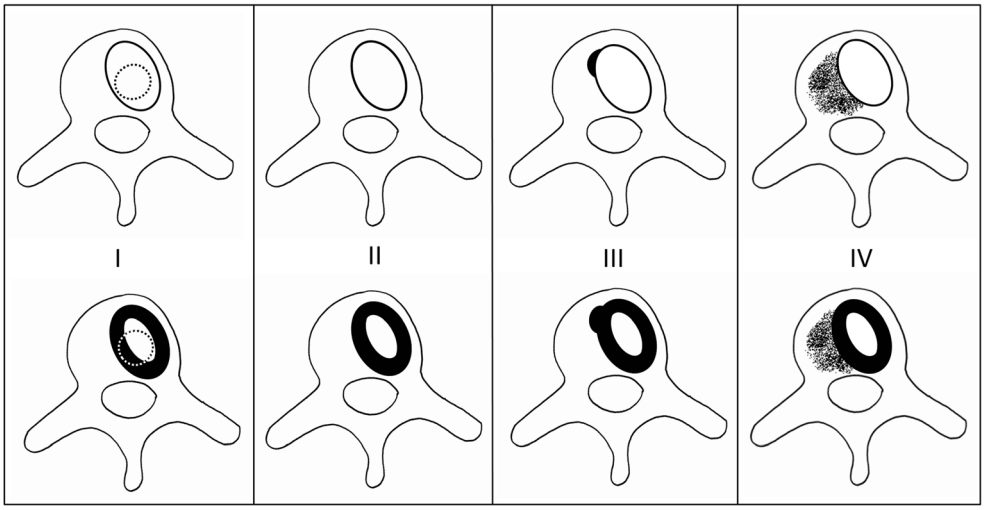

Fig. 1 Post-ablation MRI classification. Type I: ghost tumor within the external part of an oval or round-shape linear contrast enhancement; type II: oval or round-shape linear contrast enhancement; type III: nodular contrast enhancement contiguous or distant to the linear contrast enhancement; and type IV: patchy contrast enhancement contiguous or distant to the linear contrast enhancement

- *Type I* was defined as an oval or round-shape linear contrast enhancement (thin or thick) encompassing a ghost tumor, without any nodular or patchy contrast enhancement contiguous or distant to the linear contrast enhancement (Figs. 2 and 3).
- *Type II* was defined as an oval or round-shape linear contrast enhancement (thin or thick) without any ghost tumor visualized and without any nodular or patchy contrast enhancement contiguous or distant to the linear contrast enhancement (Fig. 4).
- *Type III* was defined as an oval or round-shape linear contrast enhancement (thin or thick) with a nodular contrast enhancement contiguous or distant to the linear contrast enhancement (Fig. 5b).
- *Type IV* was defined as an oval or round-shape linear contrast enhancement (thin or thick) with a patchy contrast enhancement contiguous or distant to the linear contrast enhancement (Fig. 5d).

Secondly, all post-ablation MRI were then analyzed independently by two other senior radiologists blinded of the 1-year outcome. The two readers were asked to state if the treatment was complete or incomplete, and furthermore to rank the exam according to the pre-established classification. The two secondary readers had also access to available pre-ablation MRI and per-procedural images, reflecting routine clinical practice. Results of those readings were compared to the 1-year complete treatment rate status.

Endpoints

The primary endpoint of our study was to assess the diagnostic performance of post-ablation MRI for the detection of incomplete treatment.

The secondary endpoints were the 1-year complete treatment rate and complications. Complications were reported using the Common Terminology Criteria for Adverse Events v5.0 (CTCAE) [10].

Statistical analysis

Statistical analyses were performed using EZR software version 1.35 (Saitama Medical Center, Jichi Medical University) [11]. The interobserver agreement was assessed using the unweighted Cohen's kappa (κ) and the quadratic-weighted Cohen's kappa (κw) indices of agreement [12]. The strength of agreement was defined according to Landis divisions "benchmarks" [13]. The multivariate prognostic analysis was performed using the logistic regression analysis. A two-sided p value of $< .05$ was considered significant.

Results

Patients

A total of 39 patients (24F:15M, age range 24–75 years) with 54 treated spine metastases during 41 procedures met the selection criteria. Prior to cryoablation, 32 (82.1%) received systemic treatment and 1 (2.6%) patient was treated by radiotherapy for a metastasis later treated by cryoablation for local recurrence. Primary tumor was thyroid in 16 (41.0%) patients, breast in 7 (17.9%) patients, lung in 5 (12.8%) patients, paraganglioma/pheochromocytoma in 3 (7.7%) patients, and other miscellaneous origins in 8 (20.5%) patients.

Pre-procedural imaging and cryoablation

Lesions measured 6–38 mm (mean 18.4 mm). On CT, 12 (22.2%) were sclerotic. Five (12.8%) involved part of a

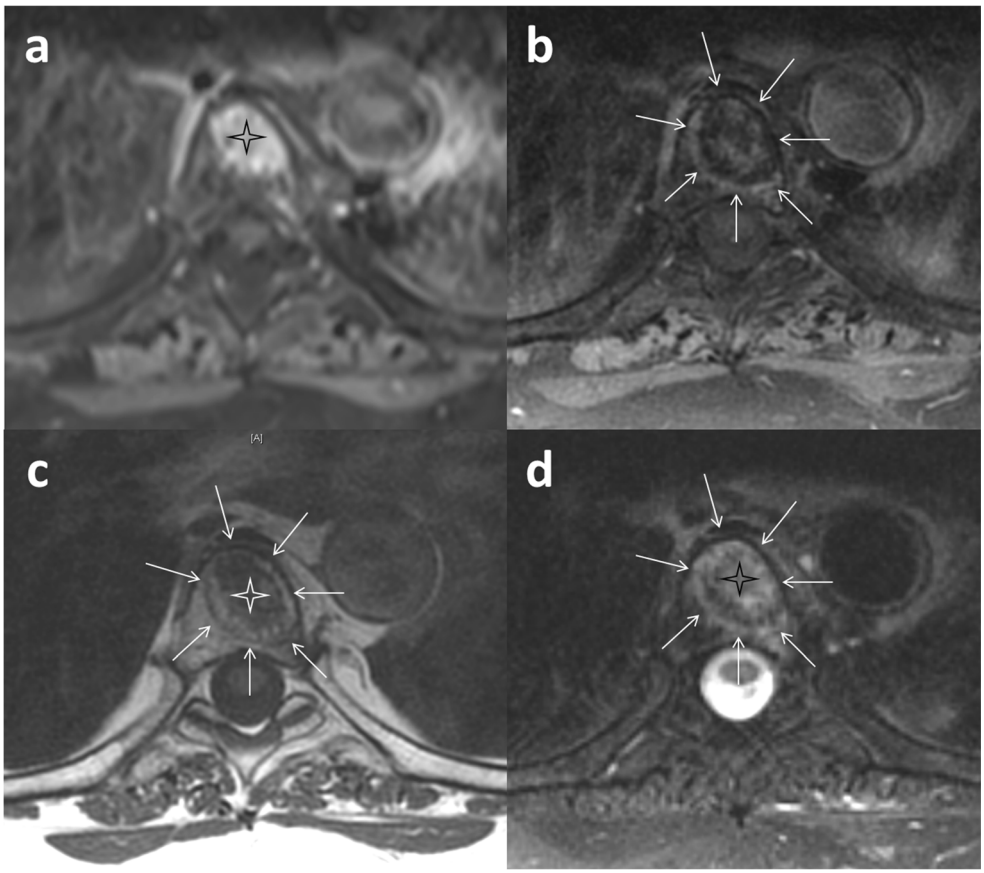

Fig. 2 Type I of the post-ablation MRI classification (first example). **a** Pre-treatment MRI with contrast-enhanced T1-weighted sequence with fat saturation showing a metastasis (cross) of a tonsil squamous carcinoma in a 70-year-old woman. **b** Post-ablation contrast-enhanced T1-weighted sequence with fat saturation showing a thin linear oval-shape enhancement (arrows). **c** Post-ablation T1-weighted sequence showing the ghost tumor with low signal intensity (cross) within the ablated zone (arrows). **d** Post-ablation T2-weighted sequence with fat saturation also showing the ghost tumor with high signal intensity (cross) within the ablated zone (arrows). No recurrence was observed at 1 year of follow-up

pedicle while the others ($N = 49$) were located only in the vertebral body. The distance from metastasis to the spinal canal ranged 0–18 mm (mean 5 mm). Twenty-three metastases showed cortical bone erosion, with soft tissue invasion in four cases. Confirmation of histology was performed with biopsy in 28 (51.2%) metastases, while the rest were presumed to be malignant metastases related to primary diagnosis, imaging appearance, and progression. A pre-procedural MRI was available in 32/39 patients with 42/53 lesions, while the remainder (7/39 patients with 9/53 lesions) only had pre-procedural CT or PET-CT.

The mean number of cryoablation performed for multiple sites per patients was 1.4 (range 1–3). Conscious sedation was performed during 31 procedures (75.6%) and general anesthesia during 10 procedures (24.4%). Epidural injection of carbon dioxide was attempted during 35 procedures (64.8% metastases) and a medullar arteriography was performed in 10 cases (18.5%) prior to the ablation. Vertebral consolidation by percutaneous vertebroplasty was performed few days later (median 15 days, range 7–255 days) in 25 cases (46.3%).

Complete treatment

The 1-year complete treatment rate per metastasis was 32 of 54 (59.3%). The results of the univariate and multivariate analyses of prognosis factors for incomplete treatment at 1-year are summarized in Table 1. In the multivariate analysis, the factors associated with a higher risk of incomplete treatment at 1-year were diameter > 25 mm ($p = .001$) and distance to the spinal canal < 2 mm ($p = .006$). For metastases measuring less than 25 mm and distant to at least 2 mm from the spinal canal, the 1-year complete treatment rate per metastasis was 23 of 24 (95.8%).

Post-ablation MRI appearance

Post-ablation MRI protocols were diverse among patients. However, all patients had at least pre-contrast T1- and T2-weighted sequences and a post-contrast T1-weighted sequence with fat saturation. In 32 cases (59.3%), post-ablation MRI showed an oval or round-shape linear enhancement, without any nodular or patchy contrast enhancement elsewhere in the vertebral body other than the needle track. This linear enhancement pattern could be thin or thick (up to 9 mm). In 22 treated metastases (40.7%), post-ablation MRI showed patchy or nodular contrast enhancement distant or contiguous to an oval or round-shape linear enhancement. The inner part of this linear enhancement had heterogeneous signal on T2-weighted sequences but had low signal intensity on T1-

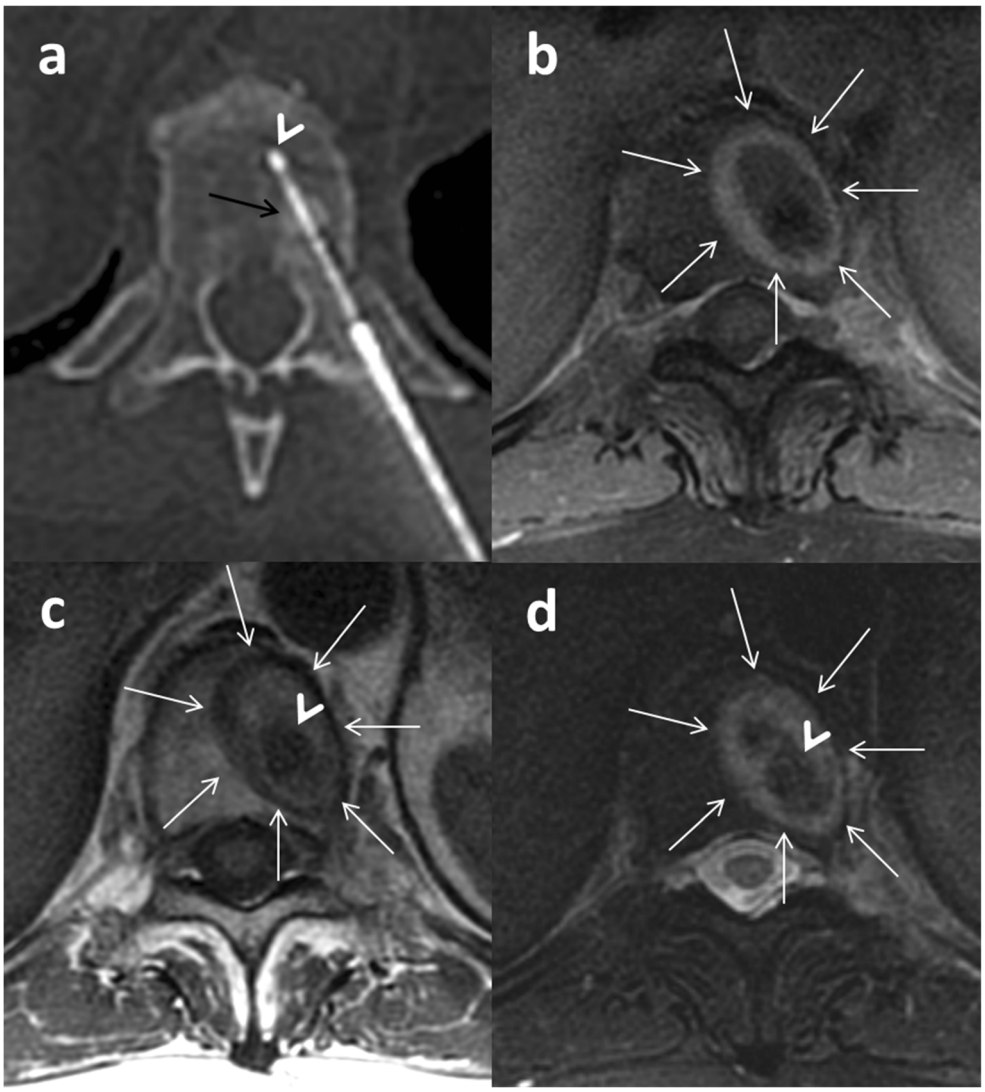

Fig. 3 Type I of the post-ablation MRI classification (second example). **a** Pre-cryoablation CT image showing the cryotherapy needle (arrow head) passing through the sclerotic metastasis (black arrow). **b** Post-ablation contrast-enhanced T1-weighted sequence with fat saturation showing a thin linear oval-shape enhancement (arrows). **c** Post-ablation T1-weighted sequence showing the ghost tumor with low signal intensity (arrow head) within the ablated zone (arrows). **d** Post-ablation T2-weighted sequence with fat saturation also showing the ghost tumor with low signal intensity (arrow head) within the ablated zone (arrows)

weighted sequences in 43 cases (79.6%). In 14 cases (25.9%), the metastasis treated was seen within external part of the linear enhancement, mainly on T2-weighted images (11 cases) with low signal intensity in 9 cases, and was referred as the ghost tumor. For the 5 remaining cases, the ghost tumors were seen on T1-weighted images with low signal intensity.

Post-ablation MRI was performed in a median time of 25 days after cryoablation (range 4 days to 4 months). For the 25 patients that had post-ablation vertebroplasty, MRI was performed in a median time of 12 days after cryoablation (range 4 to 76 days) versus 48 days (range 5 days to 4 months) for the remaining 29 patients ($p < .001$).

Performance of MRI performances for detection of incomplete treatment

Sensitivity and specificity for the detection of incomplete treatment were 77.3% (95% CI = 62.2–88.5) and 85.9% (95% CI = 75.0–93.4), respectively. Positive predictive value and negative predictive value were 79.1% (95% CI = 64.0–90.0) and 84.6% (95% CI = 73.5–92.4), respectively (Table 2). Agreement between the two readers was substantial ($\kappa = 0.69$, 95% CI = 0.50–0.89).

Performance of MRI classification

Type I was associated with a 1-year complete treatment in 100% of cases (95% CI = 77.9–100).

Type II was associated with a 1-year complete treatment in 83.3% of cases (95% CI = 69.8–92.5).

Type III was associated with a 1-year complete treatment in 35.7% of cases (95% CI = 18.6–55.9).

Type IV was associated with a 1-year complete treatment in 10.0% of cases (95% CI = 1.2–31.7).

Agreement between the two readers was substantial ($\kappa w = 0.70$, 95% CI = 0.54–0.87).

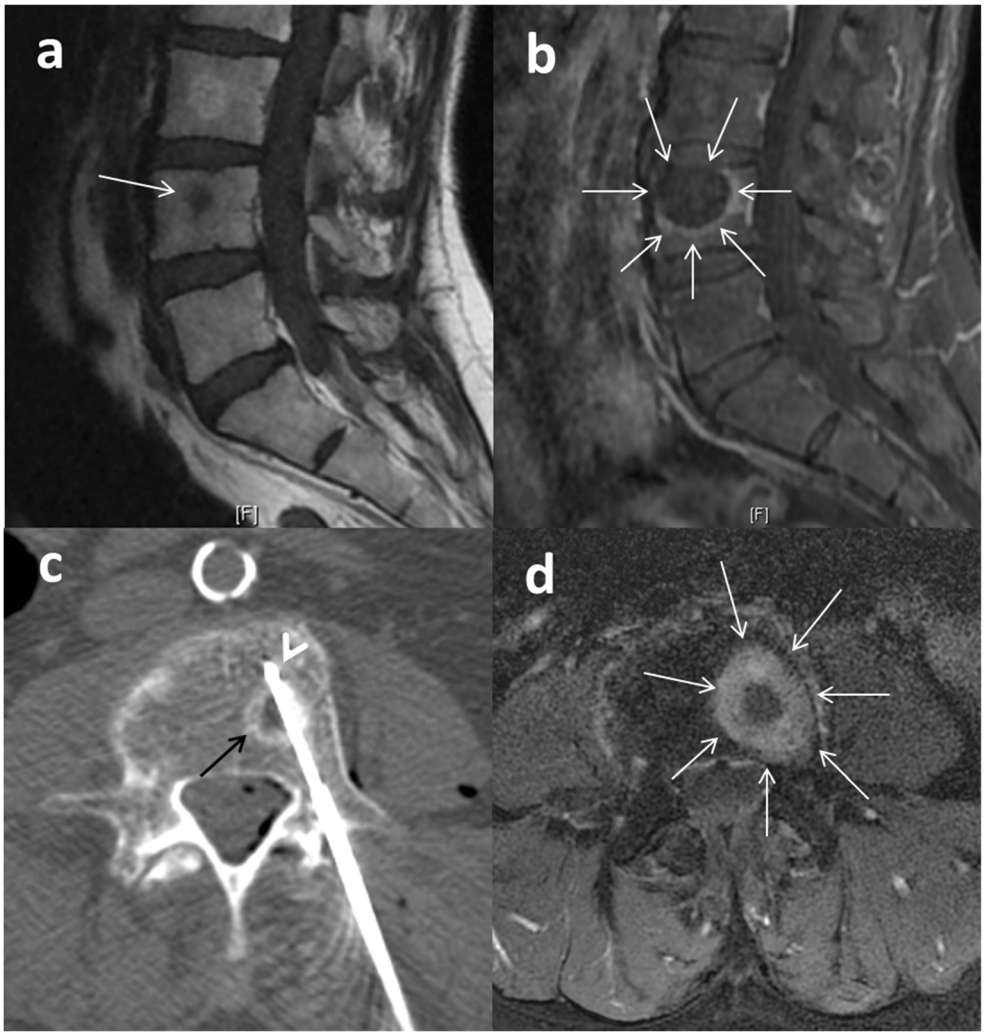

Fig. 4 Type II of the post-ablation MRI classification. **a** Unenhanced pre-ablation T1-weighted sequence showing a metastasis of 11 mm diameter (arrow) in low signal intensity on the L4 vertebra. **b** Post-ablation contrast-enhanced T1-weighted sequence with fat saturation in the same patient showing a thin linear round-shape enhancement (arrows). **c** Pre-cryoablation CT image showing a metastasis of 17 mm diameter (arrow) with the cryotherapy needle (arrow head) passing through the lesion. **d** Post-ablation contrast-enhanced T1-weighted sequence with fat saturation in the same patient showing a thick linear round-shape enhancement (arrows)

Complications

Four adverse events according to the CTCAE v5.0 were reported (two grade 3 and two grade 2). Among the grade 3 adverse events, one was a post-procedural persistent paraparesis and one was a per-procedural Tako-tsubo cardiomyopathy in a patient with metastatic functional paraganglioma. The grade 2 adverse events were transitory nerve root radiculopathy with persistent dysesthesia in one of the two cases.

Discussion

In our study, MRI performed in a median time of 25 days after cryoablation had good diagnostic accuracy to detect incomplete treatment, and the proposed classification was useful to predict incomplete ablation.

To our knowledge, CT has never been evaluated for early detection of incompletely treated spine metastases by cryoablation. CT has a lower diagnostic accuracy than MRI for bone metastases [14] and is not recommended for assessment of spinal tumor response after stereotactic body radiotherapy (SBRT) [15]. In our experience, the ablated zone in the bone was inconstantly and poorly visible on CT although it remains of great value for the assessment of bone integrity. PET-CT has shown promises in monitoring tumor response after systemic treatment for breast cancer metastatic to the bone [16, 17]. However, early post-ablation PET-CT could be limited by post-ablation inflammation at 1 month as previously shown after radiofrequency ablation of lung tumors [18].

The ablated zone can be visualized as an oval or round-shape linear contrast enhancement, thin or thick, meaning that the ablation limits are probably within the external part of the linear contrast enhancement. The ablation zone can also be seen on unenhanced images, as a low signal intensity on T1-weighted images. In some cases, the ablated metastasis can be seen inside the ablated zone, most frequently on T2-weighted sequences. Visualization of the ghost tumor within the ablated zone should be carefully sought as it gives an excellent evaluation of the ablation margins. In our study, when a ghost tumor

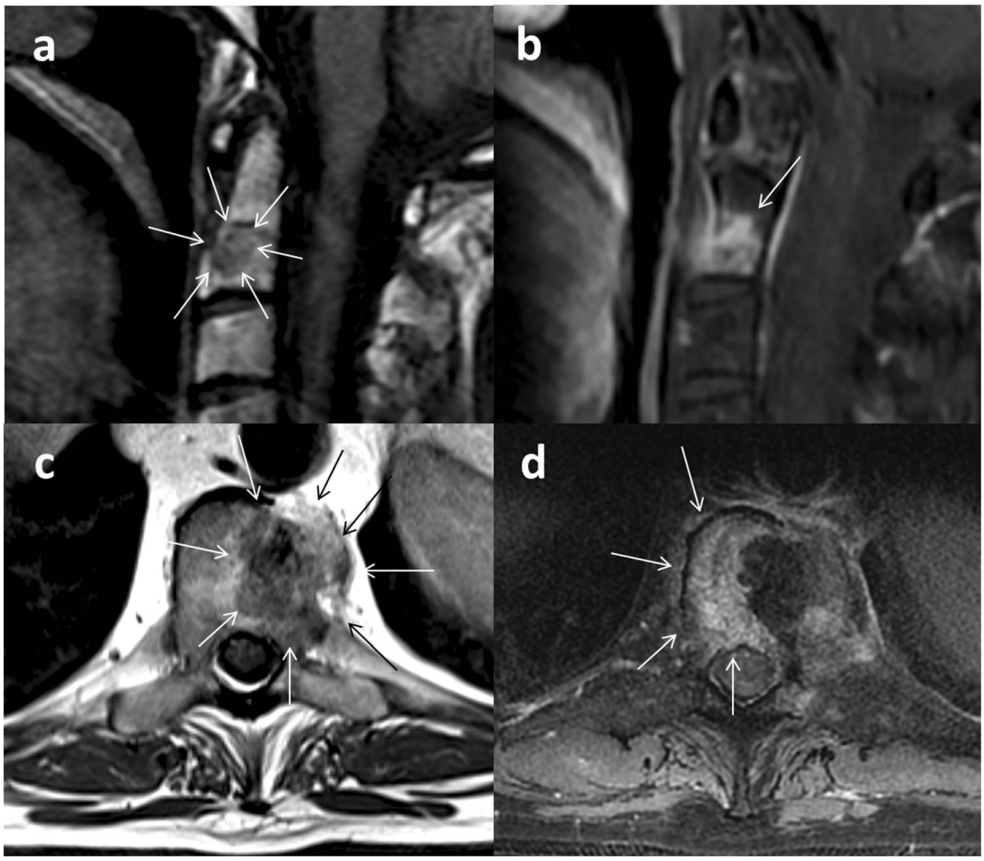

Fig. 5 Types III and IV of the post-ablation classification. **a** Unenhanced pre-ablation T1-weighted sequence showing a metastasis of 11 mm diameter (arrows) in low signal intensity on the C2 vertebra. **b** Type III of the post-ablation classification. Contrast-enhanced T1-weighted sequence with fat saturation in the same patient showing a nodular contrast enhancement (arrow) contiguous to the ablated zone. **c** Unenhanced pre-ablation T1-weighted sequence showing a metastasis on the T9 vertebra with soft tissue involvement (arrows). **d** Type IV of the post-ablation classification. Contrast-enhanced T1-weighted sequence with fat saturation in the same patient showing a patchy contrast enhancement (arrows) contiguous to the ablated zone. The pre-ablation MRI did not include a contrast-enhanced sequence probably resulting in an underestimation of the vertebral body invasion

was seen within the ablation margin (type I of the classification), no recurrence was observed at 1 year. When the ghost tumor is not visible, careful comparison with pre-treatment images should determine if the ablation zone encompasses the tumor area or not. Residual tumors appear as patchy or nodular areas with post-contrast enhancement distant or contiguous to the ablated zone. Indeed, type III and type IV of the classifications were frequently associated with incomplete treatment at 1 year. A patchy enhancement in the vertebra (type IV) was highly predictive of incomplete treatment at 1 year in our study. A pre-procedural MRI should be performed in every patient as it provides an optimal delimitation of the metastasis to be ablated and allows for the evaluation of ablation margins when comparing pre- and the post-ablation MRI.

As a result of our study, in our center, we now perform the pre-ablation MRI within a week before the ablation, and the post-ablation MRI 1 to 3 weeks after the procedure. If the post-ablation MRI is performed too soon after ablation, analysis might be hampered by post-treatment inflammation. However, it should not be delayed too much in order to limit the risk of post-treatment vertebral collapse, explaining the delay we have chosen. A 1-year MRI during the follow-up is also warranted for the definitive evaluation of local control.

Table 1 Prognostic analysis of treatment failure

	Univariate analysis		Multivariate analysis	
	OR (95% CI)	*p* value	OR (95% CI)	*p* value
Only one cryoprobe used	1.7 (0.4–6.8)	.53	0.1 (0.0–2.0)	.14
Cortical bone erosion	2.2 (0.6–8.2)	.25	1.1 (0.2–7.9)	.91
Soft tissue involvement	4.8 (0.4–264.6)	.29	14.7 (0.0–15,400.0)	.45
Procedure under conscious sedation	5.8 (1.1–60.2)	.03	2.6 (0.2–35.9)	.48
Sclerotic metastasis	2.5 (0. 6–11.8)	.19	2.2 (0.2–24.7)	.53
Proximity to the spinal canal < 2 mm	3.5 (0.1–13.5)	.04	26.3 (2.6–271.0)	.006
Size of metastasis > 25 mm	28.9 (3.5–1364.4)	< .001	377.0 (9.2–15,500.0)	.001

OR odds ratio, *CI* confidence interval

Table 2 Diagnostic performance of the post-cryoablation MRI

	Values	95% confidence interval
Sensitivity (%)	77.3	62.2–88.5
Specificity (%)	85.9	75.0–93.4
Positive predictive value (%)	79.1	64.0–90.0
Negative predictive value (%)	84.6	73.5–92.4
Diagnostic accuracy	0.8	0.7–0.9
Positive likelihood ratio	5.5	2.9–10.3
Negative likelihood ratio	0.3	0.2–0.5

The proposed post-ablation classification is a useful tool for MRI reporting. The sensitivity of MRI was average even though the specificity and the negative predictive value were good. Type I or II provided a higher degree of confidence that the ablation was complete. In these cases, a post-ablation percutaneous vertebroplasty can be pursued given the high predictive likelihood that the ablation treatment is complete. For type III, vertebroplasty should be delayed to allow prolonged and careful radiological surveillance and possibly additional locoregional treatment, such as re-treatment with cryoablation. For type IV findings, the ablation is highly likely to be incomplete and additional locoregional treatment should be performed, mainly with SBRT in association with vertebroplasty.

In our study, complete treatment at 1 year was achieved in 59.3% of cases. For metastases smaller than 25 mm and distant to at least 2 mm from the spinal canal, the 1-year complete treatment rate was achieved in 95.8% of cases, which is consistent with previously reported data on spine cryoablation by Tomasian et al [19]. However, the size of metastases and proximity to the spinal canal were not specified. Size is usually a main concern regarding percutaneous ablation techniques with an upper limit in the size of 2–3 cm [20, 21] which is consistent with our results. Proximity to the spinal canal also exposes to incomplete ablation as concerns for neurological complications may result in under-powered treatment, despite the use of nerve protective methods as carbon dioxide displacement barrier and/or peripheral nerve monitoring. However, technical success of epidural carbon dioxide injection is limited and can sometimes displace the thecal sac and the cord towards the lesion [22].

SBRT for spine metastases is a non-invasive therapeutic modality that provides good local control rates, ranging between 72 and 90% [23, 24]. Vertebral compression fractures have been reported after SBRT with an overall risk ranging from 20 to 39% [25, 26], also warranting preventive consolidation by percutaneous vertebroplasty of the vertebral body treated. Even though re-treatment by SBRT for local recurrence can be attempted in suitable patients [27], cement filling of the vertebral body will prevent any percutaneous approach. Therefore, in appropriately selected patients (i.e., metastases < 25 mm, distance from spinal canal ≥ 2 mm), we believe that percutaneous cryoablation should be considered as the first-line treatment.

We acknowledge the limitations in our retrospective study. First, even though the absence of histologic confirmation of all metastases treated may invoke some selection and outcome bias, more than half of patients had histologic confirmation, thanks to the possibility to perform a pre-procedural biopsy unlike SBRT. Secondly, our study comprises different primary tumors, and imaging follow-up modality at 1-year was heterogeneous. Finally, post-ablation MRI protocols were diverse among patient even though all patients had at least pre-contrast T1, T2-weighted sequences, and a post-contrast T1-weighted sequence with fat saturation.

In conclusion, our results suggest that post-ablation MRI is useful for the early evaluation of the ablation efficacy. We propose a classification that provides confident benchmarks for the evaluation of complete treatment at 1 year. In addition, percutaneous cryoablation seems to be a safe and effective curative treatment modality for spine metastases in appropriately selected patients (metastases < 25 mm and distance from the spinal canal ≥ 2 mm).

Funding The authors state that this work has not received any funding.

Compliance with ethical standards

Guarantor The scientific guarantor of this publication is Dr. Frederic Deschamps.

Conflict of interest The authors of this manuscript declare no relationships with any companies, whose products or services may be related to the subject matter of the article.

Statistics and biometry No complex statistical methods were necessary for this paper.

Informed consent Written informed consent was waived by the Institutional Review Board.

Ethical approval Institutional Review Board approval was obtained.

Methodology
- retrospective
- diagnostic study
- performed at one institution

References

1. Coleman RE (2006) Clinical features of metastatic bone disease and risk of skeletal morbidity. Clin Cancer Res 12:6243s–6249s
2. Fornasier VL, Horne JG (1975) Metastases to the vertebral column. Cancer 36:590–594
3. Deschamps F, Farouil G, de Baere T (2014) Percutaneous ablation of bone tumors. Diagn Interv Imaging 95:659–663
4. Munk PL, Murphy KJ, Gangi A, Liu DM (2011) Fire and ice: percutaneous ablative therapies and cement injection in management of metastatic disease of the spine. Semin Musculoskelet Radiol 15:125–134

5. Deschamps F, Farouil G, Ternes N et al (2014) Thermal ablation techniques: a curative treatment of bone metastases in selected patients? Eur Radiol 24:1971–1980
6. Gravel G, Leboulleux S, Tselikas L et al (2018) Prevention of serious skeletal-related events by interventional radiology techniques in patients with malignant paraganglioma and pheochromocytoma. Endocrine 59:547–554
7. Yang H-L, Liu T, Wang X-M et al (2011) Diagnosis of bone metastases: a meta-analysis comparing ^{18}FDG PET, CT, MRI and bone scintigraphy. Eur Radiol 21:2604–2617
8. Vanel D, Bittoun J, Tardivon A (1998) MRI of bone metastases. Eur Radiol 8:1345–1351
9. Lecouvet FE, Larbi A, Pasoglou V et al (2013) MRI for response assessment in metastatic bone disease. Eur Radiol 23:1986–1997
10. National Cancer Institute (2018) Common Terminology Criteria for Adverse Events (CTCAE). Available via https://ctep.cancer.gov/protocolDevelopment/electronic_applications/ctc.htm. Accessed 20 Sep 2018
11. Kanda Y (2013) Investigation of the freely available easy-to-use software "EZR" for medical statistics. Bone Marrow Transplant 48:452–458
12. Cohen J (1968) Weighted kappa: nominal scale agreement with provision for scaled disagreement or partial credit. Psychol Bull 70:213–220
13. Landis JR, Koch GG (1977) The measurement of observer agreement for categorical data. Biometrics 33:159–174
14. Buhmann Kirchhoff S, Becker C, Duerr HR et al (2009) Detection of osseous metastases of the spine: comparison of high resolution multi-detector-CT with MRI. Eur J Radiol 69:567–573
15. Thibault I, Chang EL, Sheehan J et al (2015) Response assessment after stereotactic body radiotherapy for spinal metastasis: a report from the SPIne response assessment in Neuro-Oncology (SPINO) group. Lancet Oncol 16:e595–e603
16. Constantinidou A, Martin A, Sharma B, Johnston SRD (2011) Positron emission tomography/computed tomography in the management of recurrent/metastatic breast cancer: a large retrospective study from the Royal Marsden Hospital. Ann Oncol 22:307–314
17. De Giorgi U, Mego M, Rohren EM et al (2010) 18F-FDG PET/CT findings and circulating tumor cell counts in the monitoring of systemic therapies for bone metastases from breast cancer. J Nucl Med 51:1213–1218
18. Deandreis D, Leboulleux S, Dromain C et al (2011) Role of FDG PET/CT and chest CT in the follow-up of lung lesions treated with radiofrequency ablation. Radiology 258:270–276
19. Tomasian A, Wallace A, Northrup B et al (2016) Spine cryoablation: pain palliation and local tumor control for vertebral metastases. AJNR Am J Neuroradiol 37:189–195
20. de Baere T, Elias D, Dromain C et al (2000) Radiofrequency ablation of 100 hepatic metastases with a mean follow-up of more than 1 year. AJR Am J Roentgenol 175:1619–1625
21. de Baère T, Aupérin A, Deschamps F et al (2015) Radiofrequency ablation is a valid treatment option for lung metastases: experience in 566 patients with 1037 metastases. Ann Oncol 26:987–991
22. Vidoni A, Grainger M, James S (2018) Experience of neuroprotective air injection during radiofrequency ablation (RFA) of spinal osteoid osteoma. Eur Radiol 10:4146–415023
23. Wang XS, Rhines LD, Shiu AS et al (2012) Stereotactic body radiation therapy for management of spinal metastases in patients without spinal cord compression: a phase 1-2 trial. Lancet Oncol 13:395–402
24. Yamada Y, Bilsky MH, Lovelock DM et al (2008) High-dose, single-fraction image-guided intensity-modulated radiotherapy for metastatic spinal lesions. Int J Radiat Oncol Biol Phys 71:484–490
25. Boehling NS, Grosshans DR, Allen PK et al (2012) Vertebral compression fracture risk after stereotactic body radiotherapy for spinal metastases. J Neurosurg Spine 16:379–386
26. Rose PS, Laufer I, Boland PJ et al (2009) Risk of fracture after single fraction image-guided intensity-modulated radiation therapy to spinal metastases. J Clin Oncol 27:5075–5079
27. Myrehaug S, Sahgal A, Hayashi M et al (2017) Reirradiation spine stereotactic body radiation therapy for spinal metastases: systematic review. J Neurosurg Spine 27:428–435